Quantum Wave-Particle Duality in Free-Electron–Bound-Electron Interaction

Bin Zhang,[1] Du Ran,[1,2,*] Reuven Ianconescu,[1,3] Aharon Friedman,[4] Jacob Scheuer,[1] Amnon Yariv,[5] and Avraham Gover[1,†]

[1]*Department of Electrical Engineering Physical Electronics, Center for Laser-Matter Interaction (LMI), Tel Aviv University, Ramat Aviv 69978, Israel*

[2]*School of Electronic Information Engineering, Yangtze Normal University, Chongqing 408100, China*

[3]*Shenkar College of Engineering and Design, 12, Anna Frank Street, Ramat Gan 5252626, Israel*

[4]*Ariel University, Ariel 40700, West Bank*

[5]*California Institute of Technology, Pasadena, California 91125, USA*

(Received 31 December 2020; accepted 8 April 2021; published 17 June 2021)

We present a comprehensive relativistic quantum-mechanical theory for interaction of a free electron with a bound electron in a model, where the free electron is represented as a finite-size quantum electron wave packet (QEW) and the bound electron is modeled by a quantum two-level system (TLS). The analysis reveals the wave-particle duality nature of the QEW, delineating the point-particle-like and wavelike interaction regimes and manifesting the physical reality of the wave function dimensions when interacting with matter. This QEW size dependence may be used for interrogation and coherent control of superposition states in a TLS and for enhancement of cathodoluminescence and electron energy-loss spectroscopy in electron microscopy.

DOI: 10.1103/PhysRevLett.126.244801

The interpretation of the quantum electron wave function $\Psi(\boldsymbol{r}, t)$ has been a matter of debate since the inception of quantum theory [1,2]. The accepted Born interpretation is that the expectation value $\langle|\Psi(\boldsymbol{r}, t)|^2\rangle$ represents the probability density of finding the electron at point $\boldsymbol{r}$ and time t. The reality of the quantum electron wave packet (QEW) and the measurability of its dimensions, as well as the transition from the quantum wave function presentation to the classical point-particle theory (the wave-particle duality) were considered previously in the context of electron interactions with light [3–10]. It was shown that the transition of the QEW radiative interaction from the wavelike regime, exhibiting characteristic multisideband photon-induced near-field electron microscopy (PINEM) energy spectrum [11–21] to the classical point-particle-like acceleration-deceleration regime [22], takes place when [3–6,23] $\Gamma = \omega\sigma_{et} = 2\pi\sigma_{ez}/\beta\lambda < 1$, where $\beta = v_0/c$ is the centroid velocity of the QEW. Namely, the transition takes place when the wave packet duration σ_{et} or its length σ_{ez} are short relative to the optical radiation period $2\pi/\omega$ or wavelength λ, respectively.

Recent technological advances enable the shaping of single QEWs in the transverse and longitudinal dimensions [24–26]. Furthermore, it has been demonstrated that the QEW density expectation value can be modulated at optical frequencies by interaction with a laser beam [17–21], and that this modulation is detectable by interaction with another synchronous laser beam, attesting to the reality of the QEW periodic sculpting (modulation) in the context of a stimulated radiative interaction [18,19,27,28]. The reality of QEW modulation features has also been asserted in the case of multiple modulation-correlated electron wave packets, where coherent superradiant emission [29], proportional to the number of electrons squared N^2, is expected [6], as in the classical case of a prebunched particle beam [30].

In analogy with the interaction of a QEW with radiation, the reality of the QEW shape and its modulation features were also claimed to be manifested in an interaction with matter in a newly proposed effect of free-electron–bound-electron resonant interaction (FEBERI) [31]. Based on a simple semiclassical model it was asserted in Ref. [31] that a QEW, passing in the vicinity of a two-level system (TLS) target (e.g., an atom, quantum dot, crystal color center, or trapped ion), would induce QEW size- and shape-dependent transitions in the TLS. Specifically, it was suggested that an ensemble of optical frequency modulated QEWs would excite resonantly TLS transitions if their frequency of modulation (produced by a laser of frequency ω_b in a PINEM setup [17]) is a subharmonic of the TLS transition frequency: $n\omega_b = \omega_{2,1} = E_{2,1}/\hbar$, where $E_{2,1} = E_2 - E_1$ is the energy gap of the TLS quantum levels. Further, it was argued that, if all QEWs are modulation correlated (by the same modulating laser), the transition rate would be enhanced in proportion to N^2 in analogy with the superradiance effect. The analogy is quite straightforward when the QEWs are in the near-point-particle limit $\Gamma = \omega_{2,1}\sigma_{et} < 1$, and injected as a periodic spatial and temporal train of pulses, a process recently termed "quantum klystron" [32] and closely related to the effect of "pulsed

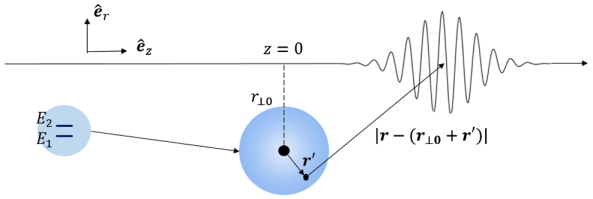

FIG. 1. Two-level system (TLS) quantum interaction model of quantum electron wave packet interaction with a bound electron.

beam scattering" [33,34]. The extension to the case of optical frequency density modulated QEWs and multiple modulation-correlated QEWs was hypothesized in Refs. [31,35] on the basis of semiclassical theory and a Born's probability interpretation of the wave function envelope modulation.

The semiclassical analysis of FEBERI and its proposed dependence on the QEW dimension were contested and caused a debate [31,36–38]. It also triggered numerous recent publications on the subject [32,35,39–42]. In this Letter we substantiate the reality of the QEW shaping in FEBERI by presenting a complete quantum-mechanical and relativistically valid formulation, demonstrating the wave packet size dependence of the FEBERI in the case of a single QEW, as well as the quantum wave-to-particle transition in this interaction. Control over the dimensions of single QEWs, and eventually over multiple modulation-correlated QEWs, may enable implementation of the FEBERI effect in new applications in electron microscopy and atomic-scale probing of quantum excitations in matter, and in diagnostics and coherent control of quantum bits (qubits) and quantum emitters.

Model.—Our comprehensive quantum-mechanical theory model is based on the configuration depicted in Fig. 1, comprising a thin free-electron QEW, propagating in the vicinity of a TLS that is modeled as a hydrogenlike atom. For simplicity we assume that the interaction of the free and bound electrons is Coulombic. We start with a Schrödinger equation for the combined wave function of the free and bound electrons

$$i\hbar\frac{\partial\Psi(\boldsymbol{r},\boldsymbol{r}',t)}{\partial t} = (H_0 + H_I)\Psi(\boldsymbol{r},\boldsymbol{r}',t), \tag{1}$$

where $H_0 = H_{0F} + H_{0B}$ is the kinetic Hamiltonian of the free and bound electrons and H_I is the interaction Hamiltonian. To apply this to relativistic electrons, we use the "relativistic" Schrödinger equation Hamiltonian for a free electron of energy $E_0 = \gamma mc^2$ and momentum $\boldsymbol{p}_0 = \gamma m\boldsymbol{v}_0$: $H_{0F}(\boldsymbol{r}) = E_0 + \boldsymbol{v}_0\cdot(-i\hbar\nabla - \boldsymbol{p}_0) + (1/2\gamma^3 m)(-i\hbar\nabla - \boldsymbol{p}_0)^2$. This Hamiltonian was derived in Ref. [3] and the Supplemental Material of Ref. [4] by a second order iterative approximation of the Klein-Gordon equation, and consequently does not include spin effects. It was also derived recently directly from the Dirac equation [43] without the quadratic term that is needed to account for electron wave packet chirp and size expansion in free drift. It corresponds to a second order expansion of the relativistic energy dispersion of a free electron: $E_p = E_0 + \boldsymbol{v}_0\cdot(\boldsymbol{p} - \boldsymbol{p}_0) + (1/2\gamma^3 m)(\boldsymbol{p} - \boldsymbol{p}_0)^2$.

The eigenfunction solutions of the bound-electron Hamiltonian are modeled as the solutions of a TLS: $H_{0B}\psi_j(\boldsymbol{r}',t) = E_j\psi_j(\boldsymbol{r}',t)$ $(j = 1,\ 2)$, where $\psi_j(\boldsymbol{r}',t) = \varphi_j(\boldsymbol{r}')e^{-iE_j t/\hbar}$. In this case the wave function of the bound electron is $\Psi_B(\boldsymbol{r}',t) = \sum_{j=1}^{2} C_j\psi_j(\boldsymbol{r}',t)$, where the coefficients satisfy $\sum_{j=1}^{2}|C_j|^2 = 1$. The wave function solution of the free-electron Hamiltonian in zero order (no interaction) is taken to be a wave packet:

$$\Psi_F^{(0)}(z,t) = \int\frac{dp}{\sqrt{2\pi\hbar}}c_p^{(0)}e^{-iE_p t/\hbar}e^{ipz/\hbar}. \tag{2}$$

We assume that the wave packet momentum distribution before interaction is a Gaussian:

$$c_p^{(0)} = \frac{1}{(2\pi\sigma_{p_0}^2)^{1/4}}\exp\left[\frac{-(p-p_0)^2}{4\sigma_{p_0}^2} - \frac{iE_p z_0}{\hbar v_0}\right], \tag{3}$$

where z_0 is the initial location of the QEW and σ_{p_0} is the QEW momentum spread. For simplicity we assume here that the QEW reaches the interaction point $z = 0$ at time t_0 at its longitudinal waist, so that the axial coordinate spread of the QEW is $\sigma_{z_0} = \hbar/2\sigma_{p_0}$ (the expansion of the QEW during the short interaction time is negligible [4]).

In this simplified model, the spin is neglected. As shown in Sec. S.1 of the Supplemental Material [44], the spin-spin interaction potential is estimated to be more than 4 orders of magnitude smaller than the Coulomb dipole interaction in the relevant regime. Furthermore, we assume that the free and bound electrons do not overlap spatially. In this case, there is no exchange energy, and we can avoid the intricate second quantization of many-body interaction theory [49]. Considering only the Coulomb interaction, we neglect the retardation effect, assuming that the electron transit time through the interaction region is much shorter than the transition frequency period [50], and the interaction Hamiltonian is (see Sec. S.2 of the Supplemental Material [44])

$$H_I(\boldsymbol{r},\boldsymbol{r}') = \frac{e^2}{4\pi\epsilon_0}\frac{\gamma\boldsymbol{r}'\cdot(\hat{\boldsymbol{e}}_z z + \hat{\boldsymbol{e}}_r r_{\perp 0})}{(\gamma^2 z^2 + r_{\perp 0}^2)^{3/2}}, \tag{4}$$

where $\boldsymbol{r}$, $\boldsymbol{r}'$ are the coordinates of the free and bound electrons, respectively. Here we used a dipole interaction Hamiltonian, under the assumption that the free electron passing by the modeled neutral hydrogen atom ($r' \ll r_{\perp 0}$), has no interaction with it other than the dipolar interaction with its electronic quantum states [42]. To keep the analysis valid in the relativistic regime, we used Feynman's

expression [51] for the Coulomb field induced by the free electron on the atom site (Sec. S.2 of the Supplemental Material [44]). In the interaction process, the expansion coefficients of the QEW [Eq. (3)] are entangled with the coefficients of the bound electron C_j, and the combined wave function is $\Psi(\boldsymbol{r}',\boldsymbol{r},t) = \sum_{j=1}^{2}\int_p dp c_{jp}(t)\varphi_j(\boldsymbol{r}')e^{-i(E_j+E_p)t/\hbar}e^{ipz/\hbar}$.

Projection onto momentum space.—After substituting the expansion of $\Psi(\boldsymbol{r}',\boldsymbol{r},t)$ into the Schrödinger equation (1) and canceling out the no-interaction terms, projection into a single momentum and TLS state results in (Sec. S.2 of the Supplemental Material [44])

$$\dot{c}_{i,p'}(t) = \frac{1}{i\hbar}\int dp\langle p', i|H_I|p, j\rangle c_{j,p'}(t)e^{-i\tilde{E}t/\hbar}, \quad (5)$$

which describes the dynamic evolution of the entangled free electron and bound electron in momentum space, where $\tilde{E} = E_p - E_{p'} - E_{i,j}$, with $E_{i,j} = E_i - E_j$. The matrix element is calculated for the specific interaction Hamiltonian (4) for longitudinally and transversely aligned dipoles (Sec. S.5 of the Supplemental Material [44]): $H_{I,i,j,\parallel}(p) = -i(e\mu_{i,j}p/\epsilon_0\gamma^2)K_0(pr_\perp/\hbar\gamma)$; $H_{I,i,j,\perp}(p) = (e\mu_{i,j}p/\epsilon_0\gamma)K_1(pr_\perp/\hbar\gamma)$, where $\boldsymbol{\mu}_{2,1} = -e\boldsymbol{r}_{2,1} = -e\int\varphi_2^*(\boldsymbol{r}')\boldsymbol{r}'\varphi_1(\boldsymbol{r}')d^3\boldsymbol{r}'$ is a dipole transition element of the bound electron, K_0 and K_1 are the zeroth and first order modified Bessel functions of the second kind, respectively.

The QEW and the TLS are disentangled before the interaction: $c_{j,p}(t_0^-) = C_j^{(0)}(t_0^-)c_p^{(0)}$. In a first order iterative approximation (Sec. S.3 of the Supplemental Material [44]), the differential equation can be solved under the approximation $c_{j,p}(t) \simeq C_j^{(0)}(t_0)c_p^{(0)}$ (stationary TLS during the interaction where t_0 is the arrival time of the QEW centroid to the TLS at $z = 0$, and t_0^- and t_0^+ are the starting and ending interaction times): $c_{i,p'}(t_0^+) = C_i^{(0)}(t_0^-)c_{p'}^{(0)} + \Delta c_{i,p'}$, where $\Delta c_{i,p'} = (2\pi/iv_0)H_{I,i,j}(p_{\rm rec})C_j^{(0)}(t_0)c_{p'-p_{\rm rec}}^{(0)}$ and $p_{\rm rec} = p' - p = -E_{i,j}/v_0$. The transition probability of the TLS after interaction is obtained by integrating the squared modulus of the combined coefficient $c_{i,p'}$ over p':

$$P_i(t_0^+) = \int_{-\infty}^{\infty}|c_{i,p'}(t_0^+)|^2dp' = P_i^{(0)} + \Delta P_i^{(1)} + \Delta P_i^{(2)}, \quad (6)$$

where $P_i^{(0)} = |C_i(t_0)|^2$ is the initial occupation probability of level i and the incremental probabilities are

$$\Delta P_i^{(1)} = 2\mathrm{Re}\left[C_i^{(0)*}(t_0)\int_{-\infty}^{\infty}dp'c_{p'}^{(0)*}(t_0)\Delta c_{i,p'}\right] = \frac{4\pi e^{-\Gamma^2/2}\sin\zeta}{v_0}|H_{I,i,j}(p_{\rm rec})| \times |C_i^{(0)*}(t_0)C_j^{(0)}(t_0)| \quad (7)$$

and

$$\Delta P_i^{(2)}(t_0^+) = \frac{4\pi^2}{v_0^2}|H_{I,i,j}(p_{\rm rec})|^2 \times |C_j^{(0)}(t_0)|^2. \quad (8)$$

In the case of excitation of a TLS from the ground state $C_2^{(0)}(t_0^-) = 0, C_1^{(0)}(t_0^-) = 1$, the excitation probability of the TLS [Eq. (8)] is given by $P_2(t_0^+) = 4\pi^2|H_{I,i,j}(p_{\rm rec})|^2/v_0^2$. Evidently the excitation probability in this case is independent of the QEW shape or dimensions [36] (see the discussion in Sec. S.4 of the Supplemental Material [44]).

However, if the TLS is initially in a superposition state, terms (7) and (8) are both present, but term $\Delta P_i^{(1)}$ [Eq. (7)] may be dominant. In the derivation of Eq. (7), we expressed $C_i^{(0)*}(t_0)C_j^{(0)}(t_0) = |C_i^{(0)*}(t_0)| \times |C_j^{(0)}(t_0)|e^{i\varphi}$ in terms of the dipole moment excitation amplitude and the phase of the superposition state (azimuth angle on the Bloch sphere) [44]. We defined the phase of the QEW arrival time relative to the TLS dipole moment excitation phase, $\zeta = \omega_{i,j}t_0 - \varphi$, and the interaction decay coefficient of the finite size QEW: $\Gamma = \omega_{i,j}\sigma_{et}$. This makes the incremental probability $\Delta P_i^{(1)}$ dependent on the wave packet dimensions for a given predetermined superposition state of the TLS, and it vanishes for a long wave packet. Instructively, Eq. (7) and the decay coefficient Γ are analogous to the decay of QEW acceleration in the transition from the classical point-particle to the quantum (PINEM) regime in a stimulated radiative interaction of a finite-size QEW [4,23].

An alternative analytic iterative solution of the Schrödinger equation for the FEBERI effect leads to general expressions for the transition probability in terms of Born's probability distribution interpretation of the QEW $\langle|\Psi_F(\boldsymbol{r},t)|^2\rangle$ (Sec. S.4 of the Supplemental Material [44]), which is conducive to further generalization to the cases of modulated multiple particle QEWs [35]. In the case of a single QEW, this approximation results in the same approximate expressions (7) and (8) in its range of validity of short QEW. To check the validity of the analytical approximations and extend the solution to any size of the QEW and a general TLS initial state, we have developed two kinds of numerical computation codes for solving the FEBERI problem in a rigorous quantum-mechanical model, starting from the momentum projection differential equation (5), or directly from the Schrödinger equation (1) (see Sec. S.7 of the Supplemental Material [44]). The computation results shown in Figs. 2–4 were performed for a model of a Gaussian QEW, showing the claimed dependence of the interaction on its size σ_{et} and delineating the transition from the quantum-wave-like limit ($\sigma_{et} > T_{2,1} = 2\pi/\omega_{2,1}$) to the point-particle-like limit ($\sigma_{et} < T_{2,1}$) of the QEW. The parameters used in the examples are typical of electron microscope PINEM-type experiments [17]: $E_0 = 200$ keV, $r_{\perp 0} = 2.4$ nm, $E_{i,j} = 2$ eV, and $\mu_{i,j} = 5$ D. To focus on the parameter

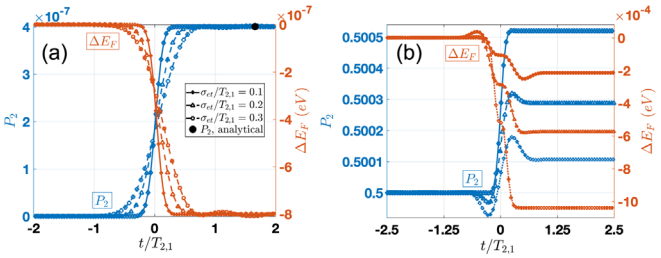

FIG. 2. Temporal evolution of excitation probability P_2 and the free-electron energy decrement ΔE_F for different σ_{et}. (a) TLS initially in the ground state. (b) TLS initially in an equatorial superposition state.

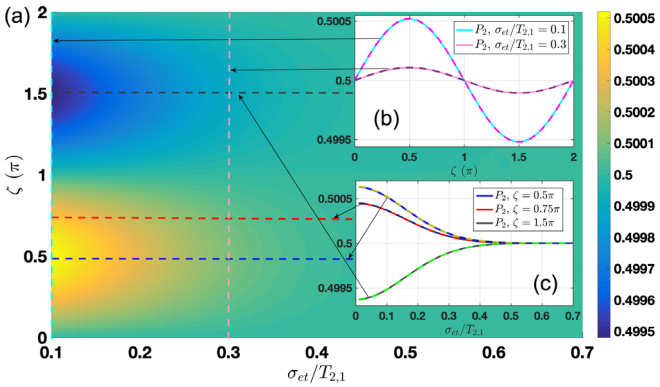

FIG. 3. (a) Numerically computed P_2 as a function of σ_{et} and ζ with the TLS initially in a superposition state. (b) Numerical (solid lines) and analytical (dashed lines) transition probability P_2 as a function of ζ for $\sigma_{et}/T_{2,1} = 0.1$ and 0.3. (c) Numerical (solid lines) and analytical (dashed lines) P_2 as a function of σ_{et} for different relative incidence phases.

scaling with the wave packet size, in all cases the transit time parameter is short relative to the QEW: $t_r = r_{\perp 0}/\gamma\beta c \ll \sigma_{et}$.

Figure 2(a) depicts the time dependence of the transition probability of the TLS, starting from the ground state, and the corresponding energy decrement of the free electron, demonstrating maintenance of energy conservation $E_F(t) - E_{F,\mathrm{in}} + \hbar\omega_{2,1}P_2 = 0$ throughout the process. The transition buildup time depends on the QEW size σ_{et}, but the postinteraction occupation probability of the upper level and the free-electron energy decrement are found to be independent of σ_{et}, in good agreement with the computed analytical expression [Eq. (8) for $|C_1^{(0)}|^2 = 1$], which is marked with a dot in the figure.

Figure 2(b) depicts the same time dependence of the transition probability of a TLS and the corresponding energy increment of the free electron, calculated for different values of σ_{et} but starting from a superposition state, taken to be $(|1\rangle + i|2\rangle)/\sqrt{2}$ (on the equator of the Bloch sphere). Unlike in the ground state case, the incremental probability for transition to the upper level strongly depends on the wave packet size in the case of a superposition state and decreases for a longer QEW, which is consistent with Eq. (7).

The strong wave-packet-size-dependent exponential decay $\exp(-\Gamma^2/2)$ predicted by the analytical approximate expression (7) is clearly demonstrated in Fig. 3 for a general superposition initial state on the equator of the Bloch sphere. The dependence on the incidence matching phase $\zeta = \omega_{2,1}t_0 - \varphi$ and on the QEW size σ_{et} is in agreement with the analytical approximate expression (7). Note the large (3 orders of magnitude) enhancement of the maximum incremental transition probability in the limit of short QEW. This is explained with a comparison of $\Delta P_2^{(1)}$ [Eq. (7)] and $\Delta P_2^{(2)}$ [Eq. (8)] that results in a relation, $[\Delta P_2^{(1)}]_{\max} = \sqrt{\Delta P_2^{(2)}}$. The total transition increment is always $\Delta P_2 = \Delta P_2^{(1)} + \Delta P_2^{(2)}$; namely, the incremental transition probability shown in Fig. 3 never decays to zero, but the contribution of $\Delta P_2^{(2)}$ is negligible. Figures 3(b) and 3(c) display the sinusoidal dependence on the incidence phase and the exponential decay with the QEW size, respectively, again in excellent agreement of the analytical and numerical results.

Finally, we present the computation of the postinteraction spectral energy distribution increment of the free electron $\Delta\rho(E) = (1/v_0)\sum_{i=1}^{2}[|c_{i,p}(t_0^+)|^2 - |c_{i,p}(t_0^-)|^2]$ for the case of a long QEW. In this case, the incidence phase dependence of the short QEW is lost, but the measurable EELS spectrum depicts a dependence on the latitudes of the TLS state on the Bloch sphere. In Fig. 4, for $\sigma_{et}/T_{2,1} = 1$, the QEW interaction with a TLS at ground state $|1\rangle$ (south pole) exhibits only energy loss (TLS excitation to upper level). At any other latitude, a PINEM-like two-sideband spectrum shifted by the recoil energy $\pm E_{2,1}$ relative to the initial energy is exhibited.

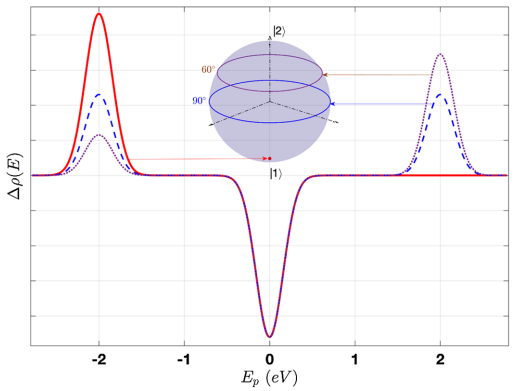

FIG. 4. EELS spectrum of long size QEWs ($\sigma_{et}/T_{2,1} = 1$) exhibiting a negative energy recoil ($-E_{2,1}$) shift single sideband for the initial TLS ground state $|1\rangle$, symmetric $\pm E_{2,1}$ sidebands for the equatorial TLS states $(|1\rangle + e^{i\varphi}|2\rangle)/\sqrt{2}$, and asymmetric net positive energy gain sidebands for initial states on the 60° latitude angle of the Bloch sphere $(|1\rangle + \sqrt{3}e^{i\varphi}|2\rangle)/2$.

The sidebands are *symmetric* on the equator, and exhibit *asymmetric* net positive energy gain spectrum for the initial TLS state in the northern hemisphere, and vice versa in the southern hemisphere.

Discussion and conclusion.—We presented a comprehensive quantum-mechanical, relativistically valid analysis of the FEBERI effect in a model in which the bound electron is represented by a TLS and the free electron is represented as a QEW. The Coulombic interaction of the two-body system was solved in terms of the relativisticly extended Schrödinger equation. Since we started from a wave packet model for the free electron, the analysis applies to the two limits of interaction, wavelike and point-particle-like cases, manifesting the wave-particle duality nature of quantum mechanics and the transition from quantum to classical point-particle presentation. This observation is similar to the analogous cases of QEW interactions with light: stimulated radiative interaction and superradiance [4–6,23]. The results show that the electron wave packet dimension is a physically observable parameter that can be measured in lab experiments by interaction with matter or light. This dependence is consistent with Born's interpretation of the quantum wave function and conducive to an extension of the process to multiple modulated QEWs, as suggested in Refs. [31,35], that would enable an enhanced resonant cathodoluminescence effect with modulation-correlated QEWs.

This Letter focused on the analysis of FEBERI with a single finite-size QEW (an extension to multiple entangled QEWs in a rigorous quantum model will be presented elsewhere). We found that the transition probability to an upper or lower quantum level of the TLS depends on its initial excitation level, and in the case of excitation from a superposition state it can be many orders of magnitude larger than the excitation from the ground state if the QEW is in the short (near point-particle) limit (typically sub–ft sec), and its arrival phase is in phase with the preset dipole oscillation phase of the TLS superposition state. Moreover, the initial quantum state of the TLS on the Bloch sphere impresses a specific signature on the EELS spectrum of the interacting electrons that depends on their size: in the short-QEW limit it displays sinusoidal phase dependent acceleration or deceleration energy shift, depending on the azimuth angle of the TLS state, and in the long QEW limit it displays a symmetric or asymmetric two-sideband spectrum that depends on the latitude angle on the northern or southern hemisphere of the TLS state on the Bloch sphere. Thus, such controlled interactions can provide diagnoses of both the QEW shape and the TLS state. In the latter case, this observation may lead to potential applications in new electron microscopy atomic-scale probing of quantum excitations in matter, and it may be particularly useful as an important application of diagnosis and coherent control of qubits and quantum emitters [42,52].

Practical implementation of these concepts requires substantial technological development and elaboration of electron microscopy techniques. Shaping the wave packet length in the range of an optical period requires development of filtering and wave packet compression techniques [26,48,53–56]. Preinteraction setting up of a single TLS target at a distinct superposition state, and measuring enough EELS data within a time period shorter than the relaxation time of the TLS, is an experimental challenge. However, there are possibilities for enhancing the measurement signal with multiple modulation-correlated QEWs [31,35,53] and with multiple TLS targets, including enhanced superradiant cathodoluminescence [57]. Many of the technical difficulties would be mitigated in scenarios of low frequency (microwave, terahertz) TLS transition frequencies, as in Ref. [32].

We acknowledge the support of ISF (Israel Science Foundation) Grant No. 00010001000 and the PBC program of the Israel Council of Higher Education.

*Corresponding author.
randu11111@163.com
†Corresponding author.
gover@eng.tau.ac.il

[1] E. Schrödinger, Phys. Rev. **28**, 1049 (1926).
[2] M. Born, Z. Phys. **38**, 803 (1926).
[3] A. Friedman, A. Gover, G. Kurizki, S. Ruschin, and A. Yariv, Rev. Mod. Phys. **60**, 471 (1988).
[4] A. Gover and Y. Pan, Phys. Lett. A **382**, 1550 (2018).
[5] Y. Pan, B. Zhang, and A. Gover, Phys. Rev. Lett. **122**, 183204 (2019).
[6] Y. Pan and A. Gover, J. Phys. Commun. **2**, 115026 (2018).
[7] H. Fares, Phys. Lett. A **384**, 126883 (2020).
[8] J. P. Corson and J. Peatross, Phys. Rev. A **84**, 053832 (2011).
[9] I. Kaminer, M. Mutzafi, A. Levy, G. Harari, H. Herzig Sheinfux, S. Skirlo, J. Nemirovsky, J. D. Joannopoulos, M. Segev, and M. Soljačić, Phys. Rev. X **6**, 011006 (2016).
[10] R. Remez, A. Karnieli, S. Trajtenberg-Mills, N. Shapira, I. Kaminer, Y. Lereah, and A. Arie, Phys. Rev. Lett. **123**, 060401 (2019).
[11] B. Barwick, D. J. Flannigan, and A. H. Zewail, Nature (London) **462**, 902 (2009).
[12] F. J. García de Abajo, A. Asenjo-Garcia, and M. Kociak, Nano Lett. **10**, 1859 (2010).
[13] S. T. Park, M. M. Lin, and A. H. Zewail, New J. Phys. **12**, 123028 (2010).
[14] S. T. Park and A. H. Zewail, J. Phys. Chem. A **116**, 11128 (2012).
[15] K. E. Echternkamp, A. Feist, S. Schäfer, and C. Ropers, Nat. Phys. **12**, 1000 (2016).
[16] G. M. Vanacore, I. Madan, G. Berruto, K. Wang, E. Pomarico, R. J. Lamb, D. McGrouther, I. Kaminer, B. Barwick, F. J. G. de Abajo, and F. Carbone, Nat. Commun. **9**, 2694 (2018).

[17] A. Feist, K. E. Echternkamp, J. Schauss, S. V. Yalunin, S. Schaefer, and C. Ropers, Nature (London) **521**, 200 (2015).
[18] K. E. Priebe, C. Rathje, S. V. Yalunin, T. Hohage, A. Feist, S. Schäfer, and C. Ropers, Nat. Photonics **11**, 793 (2017).
[19] L. Piazza, T. T. A. Lummen, E. Quiñonez, Y. Murooka, B. W. Reed, B. Barwick, and F. Carbone, Nat. Commun. **6**, 6407 (2015).
[20] M. Kozák, N. Schönenberger, and P. Hommelhoff, Phys. Rev. Lett. **120**, 103203 (2018).
[21] M. Kozák, T. Eckstein, N. Schönenberger, and P. Hommelhoff, Nat. Phys. **14**, 121 (2018).
[22] C. A. Brau, *Modern Problems in Classical Electrodynamics* (Oxford University Press, Oxford, 2004).
[23] Y. Pan and A. Gover, New J. Phys. (2021), https://doi.org/10.1088/1367-2630/abd35c.
[24] J. Verbeeck, H. Tian, and P. Schattschneider, Nature (London) **467**, 301 (2010).
[25] N. Voloch-Bloch, Y. Lereah, Y. Lilach, A. Gover, and A. Arie, Nature (London) **494**, 331 (2013).
[26] P. Baum, J. Appl. Phys. **122**, 223105 (2017).
[27] D. S. Black, U. Niedermayer, Y. Miao, Z. Zhao, O. Solgaard, R. L. Byer, and K. J. Leedle, Phys. Rev. Lett. **123**, 264802 (2019).
[28] N. Schönenberger, A. Mittelbach, P. Yousefi, J. McNeur, U. Niedermayer, and P. Hommelhoff, Phys. Rev. Lett. **123**, 264803 (2019).
[29] R. H. Dicke, Phys. Rev. **93**, 99 (1954).
[30] A. Gover, R. Ianconescu, A. Friedman, C. Emma, N. Sudar, P. Musumeci, and C. Pellegrini, Rev. Mod. Phys. **91**, 035003 (2019).
[31] A. Gover and A. Yariv, Phys. Rev. Lett. **124**, 064801 (2020).
[32] D. Rätzel, D. Hartley, O. Schwartz, and P. Haslinger, arXiv:2004.10168.
[33] F. Robicheaux and L. D. Noordam, Phys. Rev. Lett. **84**, 3735 (2000).
[34] M. S. Pindzola, M. Witthoeft, and F. Robicheaux, J. Phys. B **33**, L839 (2000).
[35] A. Gover, B. Zhang, D. Ran, R. Ianconescu, A. Friedman, J. Scheuer, and A. Yariv, arXiv:2010.15756.
[36] F. J. G. de Abajo, Phys. Rev. Lett. **126**, 019501 (2021); **126**, 069902(E) (2021).
[37] A. Gover and A. Yariv, Phys. Rev. Lett. **126**, 019502 (2021).
[38] F. J. G. de Abajo and V. Di Giulio, arXiv:2010.13510.
[39] Z. Zhao, X.-Q. Sun, and S. Fan, arXiv:2010.11396 [Phys. Rev. Lett. (to be published)].
[40] F. J. García de Abajo and V. Di Giulio, ACS Photonics **8**, 945 (2021).
[41] O. Kfir, V. Di Giulio, F. J. García de Abajo, and C. Ropers, arXiv:2010.14948.
[42] R. Ruimy, A. Gorlach, C. Mechel, N. Rivera, and I. Kaminer, arXiv:2011.00348 [Phys. Rev. Lett. (to be published)].
[43] V. Di Giulio, M. Kociak, and F. J. García de Abajo, Optica **6**, 1524 (2019).
[44] See Supplemental Material at http://link.aps.org/supplemental/10.1103/PhysRevLett.126.244801, which includes Refs. [45–48], for detailed and elaborate derivations.
[45] A. D. McLachlan, Mol. Phys. **6**, 441 (1963).
[46] Ilya Kuprov, http://spindynamics.org/documents/sd_m1_lecture_06.pdf.
[47] P. Feynman, https://www.feynmanlectures.caltech.edu/II_26.html.
[48] H. Bateman, *Tables of Integral Transforms* (McGraw-Hill, New York, 1954).
[49] R. J. Bartlett, Annu. Rev. Phys. Chem. **32**, 359 (1981).
[50] F. J. García de Abajo, Rev. Mod. Phys. **82**, 209 (2010).
[51] R. P. Feynman, R. B. Leighton, and M. Sands, *The Feynman Lectures on Physics, Mainly Electromagnetism and matter* (Addison-Wesley, Reading, MA, 1964), Vol. 2.
[52] Z. C. Shi, Y. H. Chen, W. Qin, Y. Xia, X. X. Yi, S. B. Zheng, and F. Nori, arXiv:2011.12473.
[53] V. Di Giulio and F. J. G. de Abajo, Optica **7**, 1820 (2020).
[54] Y. Morimoto and P. Baum, Phys. Rev. Lett. **125**, 193202 (2020).
[55] U. Niedermayer, T. Egenolf, O. Boine-Frankenheim, and P. Hommelhoff, Phys. Rev. Lett. **121**, 214801 (2018).
[56] O. Reinhardt and I. Kaminer, ACS Photonics, **7**, 2859 (2020).
[57] A. Halperin, A. Gover, and A. Yariv, Phys. Rev. A **50**, 3316 (1994).